HHS Public Access

Author manuscript

Cell Death Differ. Author manuscript; available in PMC 2011 March 01.

Published in final edited form as:

Cell Death Differ. 2010 September ; 17(9): 1511–1523. doi:10.1038/cdd.2010.20.

Activation of GPR30 inhibits growth of prostate cancer cells via sustained activation of Erk1/2, c-jun/c-fos-dependent upregulation of p21, and induction of G2 cell-cycle arrest

Queeny K.Y. Chan[1,*], **Hung-Ming Lam**[2,*], **Chi-Fai Ng**[3], **Amy Y.Y. Lee**[1], **Eddie S.Y. Chan**[3], **Ho-Keung Ng**[1,4], **Shuk-Mei Ho**[2,#], and **Kin-Mang Lau**[1,4,#]

[1]Department of Anatomical and Cellular Pathology, Chinese University of Hong Kong, Hong Kong.

[2]Department of Environmental Health, Center for Environmental Genetics, and Cincinnati Cancer Consortium, University of Cincinnati Medical Center, Cincinnati, Ohio, USA.

[3]Department of Surgery, Chinese University of Hong Kong, Hong Kong.

[4]State Key Laboratory in Southern China in Oncology, Chinese University of Hong Kong, Hong Kong.

Abstract

G protein–coupled receptor 30 (GPR30) exhibits estrogen-binding affinity and mediates nongenomic signaling of estrogen to regulate cell growth. We here demonstrated for the first time, in contrast to the reported promoting action of GPR30 on the growth of breast and ovarian cancer cells, that activation of GPR30 by the receptor-specific, non-estrogenic ligand G-1 inhibited growth of androgen-dependent and -independent prostate cancer (PCa) cells *in vitro* and PC-3 xenografts *in vivo*. However, G-1 elicited no growth or histological changes in the prostates of intact mice and did not inhibit growth in quiescent BPH-1, an immortalized benign prostatic epithelial cell line. Treatment of PC-3 cells with G-1-induced cell-cycle arrest at the G2 phase and reduced the expression of G2-checkpoint regulators (cyclin A2, cyclin B1, cdc25c, and cdc2) and the phosphorylation of their common transcriptional regulator NF-YA in PC-3 cells. With the extensive use of siRNA knockdown experiments and the MEK inhibitor PD98059 in the present study, we dissected the mechanism underlying G-1–induced inhibition of PC-3 cell growth, which was mediated through GPR30, followed by a sustained activation of Erk1/2 and a c-jun/c-fos-dependent upregulation of p21, resulting in the arrest of PC-3 growth at the G2 phase. The discovery of this signaling pathway lays the foundation for future development of GPR30-based therapies for PCa.

Corresponding authors: Dr. Kin-Mang Lau, Room 38018, Department of Anatomical and Cellular Pathology, Prince of Wales Hospital, Shatin, Hong Kong SAR. Tel: 852-2632-2350, Fax: 852-2637-6274, kmlau@cuhk.edu.hk; and Dr. Shuk-Mei Ho, Room 128 Kettering Complex, Department of Environmental Health, University of Cincinnati Medical Center, Cincinnati, Ohio 45267-0056, USA. Tel: 1-513-558-5701, Fax: 1-513-558-4397, Shukmei.Ho@UC.edu. [#]Kin-Mang Lau and Shuk-mei Ho are co-correspondents of this manuscript. .

[*]Queeny K.Y. Chan and Hung-Ming Lam contributed equally to the work.

Introduction

Estrogens can trigger rapid signaling responses that are initiated at the plasma membrane and mediated through activation of intracellular signaling cascades independent of nuclear translocation (1,2). Previous studies have demonstrated that ~5–10% of endogenous estrogen receptors [ERα/ERβ] and their splice variants present at the plasma membrane are responsible for the rapid estrogen signaling responses (1-5). Recently, an orphan G protein–coupled receptor (GPR30) with high-affinity and low-capacity binding to estrogens was identified at both the plasma membrane and the endoplasmic reticulum. Upon binding to ligand, GPR30 activates rapid but transient signaling of Erk1/2 to stimulate proliferation in ER-negative breast cancer cells and endometrial and ovarian cancer cells (6-12). In contrast, normal and malignant bladder urothelial cells respond to GPR30 activation with a reduction in cell proliferation (13). These findings suggest dual roles of GPR30 in the regulation of cell growth, depending on cell type. Some authors have suggested that GPR30 functions as a membranous estrogen receptor along with ERα and/or ERβ to elicit physiological estrogenic responses in the targeted cells (12,14), but contradictory data have challenged this idea (4,15-17). Thus, the biological significance of GPR30 remains unclear.

The identification of G-1 (1-[4-(6-bromobenzo[1,3]dioxol-5yl)-3a,4,5,9b-tetrahydro-3H-cyclopenta[c]quinolin-8-yl]-ethanone) as a GPR30-selective agonist (18) is a critical step towards elucidating the biological significance of GPR30, especially in cells that express ERα and/or ERβ. A previous study indicated that activation of GPR30 by G-1 stimulated proliferation in BG-1 ovarian cancer cells and SKBR3 breast cancer cells probably via induction of the expression of c-fos (11). In BG-1 cells, G-1 also upregulated the expression of cyclin D1, cyclin E, and cyclin A1 (11). SKBR3 responded to 17β-estradiol (E2) and phytoestrogens with upregulation of c-fos and stimulation of cell proliferation via GPR30, with these responses abrogated by a GPR30 antisense oligonucleotide (11,19). Findings were similar for ovarian, endometrial, and thyroid cancers in knockdown studies (9-11). Collectively, these data demonstrated that G-1 is a useful investigative tool for studying GPR30-mediated signaling.

In this study, we demonstrated the inhibitory role of GPR30 in the growth of prostate cancer (PCa) cells by investigating the effects of G-1 on an Erk1/2 kinase activation cascade that is causally linked to aberrant expression of early-response genes, upregulation of p21, and cycle arrest at the G2 phase in PCa cells, primarily using PC-3, which we found to express high levels of GPR30.

Results

G-1 induced inhibition of cell growth *in vitro* and *in vivo*

To investigate the biological effects of GPR30 activation in PCa, we treated two androgen-deprivation resistant cell lines, PC-3 (ERα- and ERβ-positive) and DU145 (predominantly ERβ-positive), for 4 days with 10^{-8} to 10^{-5} M G-1. The treatment induced a dose-dependent inhibition of cell growth in both cell lines (Figure 1A, left panel). The R_2 of goodness of fit for the sigmoid curve was 0.9947 for PC-3 cells and 0.9762 for DU145 cells. We used the IC_{50} of G-1 for PC-3 cells, 1.02×10^{-6} M, in the subsequent experiments of this study; the

IC_{50} for DU145 cells was 3.21×10^{-6} M. The difference in these IC_{50} values was statistically significant ($p<0.0001$), suggesting that PC-3 cells were more sensitive than DU145 cells to G-1. The G-1 sensitivity to the induction of cell-growth inhibition correlated with the level of expression of GPR30 (Figure 1A, right panel). Quantification of GPR30 mRNA by real-time RT-PCR analysis indicated that GPR30 expression was higher in PC-3 cells than in DU145 cells. Treatment with GPR30 siRNA significantly downregulated GPR30 mRNA expression by 7-fold (Figure 1B, left panel), and the knockdown abrogated the G-1-induced growth inhibition in PC-3 cells (Figure 1B, right panel). Similar to PC-3 and DU145 cells, the androgen-dependent LNCaP also exhibited cell growth inhibition in response to G-1 treatment (Figure S1, Supplemental Materials). Regarding nonmalignant prostatic epithelial cells, G-1 treatment only induced growth inhibition in actively proliferating BPH-1 cells grown in charcoal-stripped fetal bovine serum but not in growth-quiescent cells grown in serum-free medium (Figure S2, Supplemental Materials). The data suggest that non-malignant prostatic epithelial cells in a growth-quiescent state such as those in the normal prostate (20,21) are not responsive to G-1.

To directly investigate the effect of G-1 on normal prostatic epithelial cells *in vivo*, we treated the intact mice daily with G-1 at 4 mg/kg/day for consecutive 7 days. We compared total body and prostate weights, and histology of two prostatic lobes (dorsolateral and ventral prostates) in the treated animals with control mice treated with vehicle alone (2.5% DMSO, 5% ethanol). No significant difference was observed in total body and prostate weights of G-1-treated mice when compared to controls (Figure S3, Supplemental materials). Moreover, no histological changes such as height/size of luminal epithelial cells and architecture of acini were observed in both prostatic lobes of the G-1 treated mice. These findings indicate that normal prostatic epithelial cells *in vivo* are not responsive to G-1-treatment.

Results of quantitative RT-PCR analysis on 7 pairs of clinical prostate cancer samples and their corresponding adjacent normal tissues showed a trend of slight reduction in GPR30 transcript levels in cancers ($p = 0.1288$), similar to the finding based on the public DNA microarray database from Oncomine (Figure S4, Supplemental Materials). However, further study of GPR30 protein expression in a large cohort of samples is needed to verify the apparent reduction. Nevertheless, the majority of PCa in patients expressed GPR30.

We next examined the effects of G-1 on anchorage-independent growth of PC-3 cells using a 1-week 96-well soft-agar growth assay (22) (Figure 1C). The treatment of PC-3 cells with G-1 significantly reduced the ability of the cells to form colonies in soft agar, but cells treated with the vehicle control did not have this response. However, the GPR30-siRNA, but not a scramble siRNA, was able to block the G-1–induced growth inhibition in PC-3 cells. These data provide direct evidence that G-1–induced inhibition of the growth of PC-3 cells is dependent on the expression of GPR30.

The PC-3 xenograft model was used to evaluate the effects of G-1 on PCa growth *in vivo*. Nude mice bearing PC-3 xenografts were treated daily with G-1 or the vehicle control, and the tumor was measured at 4-day intervals. Treatment with G-1 significantly suppressed the growth of the xenografts over the entire treatment period, as compared with treatment with

vehicle (Figure 1D). The tumors in the vehicle-treated mice grew 3.8-fold over this period, whereas those in the G-1–treated animals only doubled in size (Figure 1D, left panel). After the tumors were removed, the body weights of the vehicle- and the G-1–treated mice were determined and found to be the same, suggesting that G-1 was minimally toxic in nude mice (Figure 1D, right panel).

Because PC-3 cells express both ERs, we conducted this experiment to rule out the possibility that G-1–induced growth inhibition is mediated by one of these receptors. PC-3 cells were treated with G-1 in the absence or presence of a specific receptor antagonist. Treatment of PC-3 with 1 μM G-1 alone induced a significant reduction in cell growth (Figure 1E). The co-treatment of PC-3 cells with G-1 and a specific ER antagonist (1 μM) including ICI 182,780 fulvestrant (an ERα and ERβ antagonist), MPP dihydrochloride (an ERα antagonist), and PHTPP (an ERβ antagonist) was unable to reverse the G-1–induced growth inhibition, suggesting that G-1 action is not mediated via one of these receptors. As we previously reported in one of our studies (23), treatment of PC-3 cells with ICI alone caused a 20% reduction in cell growth, whereas treatment with MPP dihydrochloride and PHTPP had no effect. PC-3 cells were also treated with the estrogen estradiol-17β (E2) (10^{-9}–10^{-6} M), and minimal or no inhibition of PC-3 cell growth was observed (data not shown), a finding similar to our previous reports (23). Moreover, a similar cell growth inhibition was induced by co–treatment with G-1 and E2, indicating that E2 had no synergistic or blocking effect on G-1–induced cell growth inhibition in PC-3 cells (Figure S4, Supplemental Materials).

G-1 induced a persistent cell-cycle arrest at the G2 but not the mitotic phase of the cell cycle

Flow cytometry analysis (Figure 2A and Figure S5, Supplemental Materials) showed a significant increase in the number of cells in the G2/M phase following treatment of PC-3 cells with G-1 for 1 day, compared with cell populations in samples from ethanol-treated controls. The increase lasted throughout the four-day treatment, indicating induction of a persistent cell-cycle arrest in the G2/M stage of the cell cycle by G-1 in PC-3 cells. Prolonged G2/M arrest by G-1 eventually resulted in induction of apoptosis, as the sub–G1 cell populations and Annexin V–positive stained cells increased after treatment for 3 and 4 days (Figure S5 and S6, Supplemental Materials). Similar G2/M arrest by G-1 was also observed in LNCaP cells (Figure S7, Supplemental Materials).

To determine whether the G-1–treated PC-3 cells were arrested at the G2 or the mitotic phase, we examined changes in the expression of a panel of cell cycle–specific markers over time (Figure 2B). The two mitotic phase markers, phosphorylated Bcl-2 and MPM-2, either were not expressed or showed no significant change in expression levels over time (Figure 2B). In contrast, expression levels of G2-checkpoint regulators, including cyclin B1, cyclin-dependent kinase 1 (cdc2) and its phosphorylated proteins, and cdc25C were significantly downregulated in PC-3 cells treated with G-1 over a 72-h period. In addition, the level of cyclin A2, which functions in the transition from both G1 to S and G2 to the mitotic phase of the cell cycle, also decreased; however, the expression of cyclin E, which is involved in the transition of G1 to S, did not change. In agreement with changes in the protein level,

expression of mRNAs of cyclin B1, cdc2, cdc25C, and cyclin A2, but not that of cyclin E, was also significantly downregulated by treatment with G-1 at various time points, as determined quantitatively by real-time RT-PCR analysis (Figure 2C). Collectively, these data support the notion that G-1 treatment induced cell-cycle arrest at the G2 phase of the cell cycle in PC-3 cells. Our observation that G-1 reduced the phosphorylation of NF-YA, but did not change NF-YA protein level *per se*, in PC-3 cells (Figure 2D) further supports previous reports that NF-YA regulates the transcriptional expression of G2 checkpoint regulators via binding to the CCAAT motif in their promoters (24-26).

G-1 induced a sustained GPR30-dependent Erk1/2 phosphorylation and nuclear accumulation, and the mitogen-activated protein kinase kinase (MEK) inhibitor PD98059 reversed the G-1–induced growth inhibition

Treatment of PC-3 cells with 1 μM G-1 over a 3-day period induced a sustained increase in the level of phosphorylated Erk1/2 but did not change the level of total Erk1/2 protein (Figure 3A, upper panels). The earliest time point at which Erk1/2 phosphorylation became noticeable is after 1 h of G-1 treatment (Figure 3A, lower panel). Such induced phosphorylation was also found in G-1–treated LNCaP cells (Figure S8, Supplemental Materials). The G-1–induced phosphorylation of Erk1/2 in PC-3 cells was then shown to be mediated by GPR30, as transfection of a GPR30-siRNA into these cells, but not of a scrambled siRNA control, abrogated the G-1 action (Figure 3B).

Upon activation, the phosphorylated Erk1/2 translocates from the cytoplasm to the nucleus to trigger transcriptional activation of its downstream nuclear targets (27-29). In this study, we compared the effects of G-1–induced nuclear accumulation of phosphorylated Erk1/2 in PC-3 cells and MCF-7 breast cancer cells. In a temporal study, using immunofluorescence staining of the phosphorylated form of Erk1/2 in cells, we observed a time-dependent increase in nuclear localization of phosphorylated Erk1/2 in G-1–treated PC-3 cells that lasted for at least 24 h (Figure 3C). In contrast, G-1–induced nuclear accumulation of phosphorylated Erk1/2 in MCF-7 cells peaked at 1 h after treatment and rapidly declined to undetectable levels by 24 h (Figure 3C).

Last, treatment of PC-3 cells with 30 μM of the MEK inhibitor PD98059 blocked the G-1–induced inhibition of cell growth (Figure 3D), suggesting that the inhibitory effect of G-1 on PCa cell growth could be mediated through the induction of Erk1/2 activation, which is downstream of MEK. The treatment of PC-3 cells with PD98059 and LY294002 alone did not elicit any significant alteration in cell growth (data not shown). However, the phosphoinositide 3-kinases (PI3Kinases) inhibitor LY294002 cannot block the G-1–induced cell growth inhibition (Figure 3D), suggesting that PI3Kinases–mediated pathway may not be involved.

G-1 induced p21 expression via GPR30-mediated signaling to inhibit cell growth

The treatment of PC-3 cells with G-1 markedly increased p21 expression at both the mRNA and protein levels in a dose- and time-dependent manner (Figure 4A). Similarly, LNCaP upregulated p21 in response to G-1 (Figure S8, Supplemental Materials). The G-1–induced upregulation of p21 is mediated via GPR30, since GPR30 siRNA, but not a scramble siRNA

control, completely abolished the G-1 effect on p21 expression (Figure 4B). We then investigated the role played by p21 upregulation in the inhibitory effect of G-1 on PCa cell growth. PC-3 cells were transfected with a p21 siRNA or a scramble siRNA control. The former transfection effectively blocked the G-1–induced overexpression of p21 protein, but the latter did not (Figure 4D, fourth panel). Importantly, the siRNA-mediated inhibition of p21 overexpression in G-1–treated PC-3 cells also abrogated the growth inhibitory action of G-1 on these cells (Figure 4C). In line with this abrogation, this knockdown also prevented the G-1–induced downregulation of cyclin B1, cdc25c, and cdc2 expression in the cells (Figure 4D). Our earlier experiments clearly demonstrated that the G-1–induced growth inhibition in PC-3 cells was accompanied by the downregulation of these G2-checkpoint regulators (Figure 2). Taken together, these findings support the notion that G-1, via GPR30 activation, upregulates p21 and that the upregulation of p21 is required for the manifestation of the G-1–induced growth inhibition in PC-3 cells.

Obliteration of G-1-induced p21 upregulation by MEK inhibitor PD98059

Treatment with 1 μM G-1 for 48 h substantially induced phosphorylation of Erk1/2 and upregulation of p21 expression in PC-3 cells. Pretreatment with 30 μM PD98059 obliterated the inductive effects of G-1, as this inhibitor completely abolished p21 upregulation and Erk1/2 phosphorylation in the cells (Figure 4E). These findings suggested that phosphorylation of Erk1/2 was essential for the upregulation of p21 expression in G-1-treated PC-3 cells.

G-1 upregulated the expression and phosphorylation of two early-response genes (c-jun and c-fos) and phosphorylation of their upstream regulators

Serum and growth factors are potent activators of Erk1/2 to stimulate activator protein-1 (AP-1) complex, which is composed of two early-response gene proteins, c-jun and c-fos (30,31). Treatment with 1 μM G-1 for 24 h significantly induced c-jun and c-fos mRNAs and proteins as compared with controls, in which c-jun and c-fos proteins were undetectable (Figure 5A).

Expression of c-jun is self-regulated (32,33), and phosphorylation of c-jun activates its transcriptional ability, leading to the induction of c-jun (34,35). We found that treatment with 1 μM G-1 for 24 h induced the phosphorylation of c-jun and c-fos (Figure 5B). Pretreatment with 30 μM PD98059 prior to the 24-h treatment with G-1 significantly reduced the induction of phosphorylated c-jun and phosphorylated c-fos, whereas cells not pretreated with the inhibitor expressed high levels of phosphorylated c-jun and phosphorylated c-fos when treated with G-1 (Figure 5B).

Gupta and Prywes (36) demonstrated that epidermal growth factor (EGF) induced upregulation of c-jun expression through the phosphorylation of MSK1 and ATF1. PC-3 cells treated with 1 μM G-1 for 24 h expressed high levels of phosphorylated MSK1 and phosphorylated ATF1, but controls did not (Figure 5C). These findings suggested that G-1 treatment can also stimulate phosphorylation of MSK1 and ATF1 followed by the upregulation of c-jun expression in PCa cells. With regard to the upstream regulator of c-fos, G-1 treatment substantially induced phosphorylation of Elk-1 (Figure 5C).

Involvement of c-jun and c-fos in the G-1–induced upregulation of p21 and downregulation of cyclin B1 but not in the phosphorylation of Erk1/2

This study was conducted to demonstrate that the G-1–induced upregulation of p21 is mediated by overexpression of the early-response genes c-jun and c-fos and that this cascade is causally linked to the G-1–induced inhibition of growth of PC-3 cells. G-1 treatment induced c-jun and c-fos expression along with upregulation of p21 and downregulation of cyclin B1 in PC-3 cells, as described above. siRNA knockdown of either c-jun or c-fos alone (Figure 6A) blocked the G-1–induced cell-growth inhibition (Figure 6B). In addition, double siRNA knockdown of c-jun and c-fos completely reversed the inhibitory effect of G-1 on cell growth (Figure 6B). Consistent with our hypothesis that the induction of c-jun and c-fos were the downstream targets of G-1–induced Erk1/2 activation in PC-3 cells, siRNA knockdown of c-jun or c-fos did not affect the phosphorylation of Erk1/2 by G-1 (Figure 6C). However, the knockdowns abolished the upregulation of p21 and downregulation of cyclin B1 in these cells (Figure 6C), indicating that p21 and a G2-checkpoint regulator are downstream of these early-response genes. Collectively, findings from these experiments indicated that upregulation of c-jun or c-fos is downstream of Erk1/2 activation but upstream of p21 upregulation.

Discussion

We here report that the activation of GPR30 by the receptor-specific, non-estrogenic ligand G-1 led to growth inhibition of PCa cells (PC-3, DU145, LNCaP) in culture and as xenografts (PC-3) in nude mice. This finding is in stark contrast to the growth-promoting action of G-1 mediated by GPR30 activation in breast, endometrial, ovarian, and thyroid cancer cell lines (6, 9-11, 19). Furthermore, we found G-1 to have little or no effects (weight and histology) on mouse prostate and on growth-quiescent immortalized benign prostatic epithelial cells in cultures. As depicted in Figure 7, the steps involved in the G-1-induced, GPR30-mediated growth inhibitory cascade in PCa cells were empirically validated by a comprehensive series of siRNA knockdown experiments and the MEK inhibitor PD98059. In PC-3 cells, G-1, through GPR30 activation, caused a prolonged activation and nuclear accumulation of Erk1/2. G-1 also activated the early-response genes c-jun and c-fos, leading to upregulation of p21, which in turn downregulated a number of key G2-checkpoint regulators and ultimately led to cell-cycle arrest at the G2 phase in PC-3 cells.

Previous studies by us (23) and others (37) demonstrated that both ICI and E2 inhibited PC-3 cell growth in a modest manner. Because PC-3 expresses both ER-α and ER-β, as well as GPR30, it is difficult to pinpoint which of the three receptors is responsible for mediating the growth inhibitory action of the antiestrogen/estrogen. However, E2 was shown to have a 15-fold higher affinity for ER-α and ER-β than for GPR30 (18). Thus, it is thought that the action of ICI/E2 is mediated largely via the transactivation of the ERs rather than GPR30 in PC-3 cells. To study the specific effect of GPR30 in ER-positive PC-3 cells, we used G-1, which is a selective ligand for GPR30, in the present study. G-1 has little to no affinity for the two ERs (18), suggesting that the inhibition of PC-3 cell growth is attributable primarily to the activation of GPR30. This premise was confirmed by siRNA knockdown of GPR30, which effectively blocked the inhibitory effects of G-1 on PC-3 cell growth. Furthermore,

G-1 is unlikely to act through ERs, since the blockade of ER action by specific antagonists (ICI, MPP dihydrochloride, PHTPP) did not alter the growth inhibitory effects of G-1 on PC-3 cells.

The mode of action of G-1 and its interaction with GPR30 in PCa cells has not been studied previously. In contrast, much is known about breast cancer cells. For example, the exposure of the ER-negative breast cancer cell line SKBR3 to estradiol-17β promoted a rapid activation of mitogen-activated protein kinases Erk1/2 (<0.5 h) and stimulated cell growth (6, 11) and cell migration (38) in a GPR30-dependent manner. In the present study, G-1 also induced Erk1/2 activation in PC-3 cells, but the biological consequence was a profound inhibition of cell growth. Both Erk1/2 activation and cell-growth inhibition were dependent on GPR30, since siRNA knockdown of the receptor effectively blocked these responses. In addition, the G-1–induced Erk1/2 activation and cell-growth inhibition were both suppressed by the MEK inhibitor PD98059, indicating that the kinase is the common upstream regulator. In human umbilical vein smooth muscle cells, G-1 exerted a similar biological action by inducing Erk1/2 activation and cell-growth inhibition (39).

At this point we do not know why G-1 activation of GPR30 induces opposite effects on cell growth in different cell types, but these differences may be related to the duration of nuclear occupancy of activated Erk1/2. Upon activation, the phosphorylated Erk1/2 translocates from the cytoplasm to the nucleus to phosphorylate their nuclear targets for transcripitional regulation (27-29). It has been proposed that signal duration of Erk1/2 activation could dictate a cell-fate decision (40), with transient Erk1/2 activation leading to cell survival and proliferation and sustained activation with nuclear accumulation of activated Erk1/2 transmitting antiproliferative signals (40-44). A previous study reported that the differences between cell-growth responses of osteoclasts/osteocytes and osteoblasts to estrogens depend on the kinetics of Erk1/2 activation and duration of nuclear accumulation of phosphorylated Erk1/2 (43). In the present study, we showed that the G-1–induced Erk1/2 activation in PC-3 cells was rapid but unusually prolonged (≥ 24 h) as compared with that induced in MCF-7 cells, which peaked at 1 h and vanished by 24 h. Whether the signal duration of Erk1/2 activation is central to the PCa cell-growth response to G-1 needs to be investigated in future studies to clarify the role of GPR30 in cell-fate determination.

The cell-cycle regulator p21 was originally thought to inhibit cell-cycle progression in the G1 phase, but recent evidence indicates that it is also involved in G2/M arrest (45). Upregulation of p21 has been shown to associate with nuclear translocation of G2 checkpoint regulators, including cyclin B, and the formation of the cyclin B/cdc2 and cyclin A/CDK2 complex (46). In fact, the demonstration that upregulation by Erk1/2 activation resulted in G2/M arrest was noted in in NIH 3T3 and HeLa cells (47,48), and an association between p21 induction and decreases of cyclin B and cdc25C contributed to G2/M arrest (48-50). Here we reported that the G-1–induced inhibition of PC-3 cell growth occurred specifically at the G2 phase, accompanied by a marked elevation of p21 expression, in a GPR30-dependent manner. Furthermore, we observed a significant downregulation of several G2-specific checkpoint proteins (e.g., cyclin B1, cdc2, and cdc25C) in G-1–treated cells. One mechanism by which p21 upregulation can suppress multiple G2 checkpoint regulators is by inhibiting the phosphorylation of the nuclear factor Y A subunit (NF-YA),

which binds to a common CCAAT motif in these proteins (51-53). Indeed, we observed a significant reduction in NF-YA phosphorylation after G-1 treatment. Finally, we found siRNA knockdown of p21 effectively ameliorated the G-1–induced inhibition of cell growth and reversed the downregulation of G2 checkpoint modulators. Taken together, these findings provide credence for p21-mediation of the G-1–induced cell-cycle arrest at the G2 phase in PC-3 cells.

We further investigated the mechanism underlying GPR30-mediated p21-induced growth inhibition in PC-3 cells. Kardassis et al. (54) demonstrated that c-jun transactivated the p21 gene promoter. This finding prompted us to ascertain if the G-1–induced upregulation of p21 is caused by an enhancement of expression or by an increased activation of the early-response genes. We found that c-jun and c-fos were upregulated and activated in G-1–treated PC-3 cells. Furthermore, our study also demonstrated that the transcriptional factors MSK1 and ATF1 that activate c-jun, as well as Elk-1 that activates c-fos (36), were phoshosphorylated in G-1–treated cells. Knockdown of each of the early-response genes with small interfering RNA blocked p21 upregulation, cyclin B downregulation, and growth inhibition induced by G-1 in PC-3 cells. Collectively, these data support the mediation of G-1–induced p21 upregulation via the activation of the early-response genes c-jun and c-fos in PC-3 cells. This conclusion is substantiated by the observation that the MEK inhibitor PD98059 was able to block the activation of c-jun, c-fos, and p21 upregulation in G-1–treated PC-3 cells.

Our data showed that GPR30 was expressed in variable but detectable levels in PCa tissues and cell lines, and G-1 induced cell growth-inhibition in both androgen-responsive (e.g. LNCaP) and androgen-deprivation-resistant (e.g. PC-3) PCa cells *in vitro* and *in vivo*. The treatment was found to have minimal or no effects on normal prostatic epithelial cells in the mouse prostate and on benign prostate epithelial cells (e.g. BPH-1) arrested in a growth-quiescent state, which is the state most normal epithelial cells are in *in vivo* (20,21). Therefore, this agent may have the potential to be used alone or in combination with androgen-deprivation therapies as first-line treatment regimens for advanced PCa, local or metastatic. The treatment is likely to pose little or no harmful effects on normal prostatic tissues in patients. Additionally, it may add efficacy when used in conjunction with standard chemotherapies for metastatic PCa.

In conclusion, we demonstrated that treatment of PCa cells with G-1 induced growth inhibition *in vitro* and *in vivo* via the activation of GPR30 and cell-cycle arrest at the G2 phase. We further provided evidence supporting a novel G-1/GPR30 signaling pathway that involves a protracted activation of Erk1/2 that is linked to a c-jun- and c-fos–mediated increase in p21 expression. The discovery of this signaling pathway opens up new opportunities for the development of GPR30-based therapies for PCa by using G-1 or its derivatives.

Materials and Methods

Analysis by reverse transcription-polymerase chain reaction (RT-PCR)

Total RNA samples were reverse-transcribed using Moloney-murine-leukemia-virus reverse transcriptase and random hexamer (Applied Biosystems, Foster City, CA). Primer sequences are presented in Table S1 (Supplemental Materials). PCR reactions with SYBR Green PCR Master-Mix (Applied Biosystems) were monitored in real time with iCYCLER (Bio-Rad Laboratories, Hercules, CA). Cycle thresholds (C_T) of the genes of interest were compared with those of ribosomal protein 3 (RPS3) to determine relative expression levels (55). Relative fold changes between the expression of the genes of interest in treated and control samples were determined by the equation: fold change = $2^{-[\Delta\Delta CT]}$, where $\Delta\Delta C_T = (C_{T\ \text{gene of interest}} - C_{T\ RPS3})_{treated} - (C_{T\ \text{gene of interest}} - C_{T\ RPS3})_{control}$.

Cell-growth assay

Effects of G-1 (Cayman, Ann Arbor, MI) treatment on PCa cell growth were determined by the MTT (3-[4,5-dimethylhiazol-2-yl]-2,5-diphenyltetrazolium bromide) assay; 1.5×10^3 cells per well were seeded in RPMI1640 medium supplemented with 5% charcoal-stripped fetal bovine serum (CS-FBS) as day 0. After 24 h, the cells were treated with 1×10^{-8}, 2×10^{-7}, 4×10^{-7}, 6×10^{-7}, 8×10^{-7}, 1×10^{-6}, 4×10^{-6}, 6×10^{-6}, 8×10^{-6}, and 1×10^{-5} M G-1 in 0.1% ethanol for 4 days in octuplicate; control cells were treated with drug vehicle (0.1% ethanol). Growth of the sample at various time points relative to that of the day 1 control was calculated by the formula $(OD_{sample} - OD_{blank})/(OD_{Day\ 1control} - OD_{blank})$, and the relative growth of the day 1 control was set as 1. The concentration of G-1 (IC_{50}) that achieved 50% inhibition of cell growth was calculated from absorbance values on day 4.

In a set of experiments, PC-3 cells (American Type Culture Collection, Manassas, VA) were treated with a nuclear receptor antagonist (1 μM) or kinase inhibitors (PD98059 or LY294002) either alone or with G-1. The antagonists used included ICI 182,780 or fulvestrant (an ERα and ERβ antagonist, a gift from Zeneca Pharmaceuticals, Cheshire, UK), 1,3-bis(4-hydroxyphenyl)-4-methyl-5-[4-(2-piperidinylethoxy)phenol]-1H-pyrazole (MPP dihydrochloride; an ERα antagonist, Tocris, Ellisville, MO), and 4-[2-phenyl-5,7-bis(trifluoromethyl)pyrazolo[1,5-a]pyrimidin-3-yl]phenol (PHTPP; an ERβ antagonist, Tocris, Ellisville, MO).

Flow cytometry analysis

PC-3 cells were cultured overnight in RPMI1640 medium supplemented with 5% CS-FBS and then treated with 1 μM G-1 for 1–4 days. The treated cells were fixed and stained with propidium iodide. At least 20,000 stained cells were analyzed by FACSAria (Becton Dickinson-Biosciences, Franklin Lakes, NJ).

Treatment of GPR30, p21 (p21), c-jun, or c-fos siRNAs

PC-3 cells (2×10^5) were cultured in 4 ml of RPMI1640 medium supplemented with CS-FBS and 1 ml of siRNA-Lipofectamine-2000 mixture (40 nM siRNA for GPR30, p21, c-jun, or c-fos) and 10 μl Lipofectamine-2000 in Opti-MEM I medium) (Invitrogen, Carlsbad, CA). The siRNA-treated cells were treated with 1 μM G-1 for another 2 days and then

subjected to real-time RT-PCR and Western blot analysis. The predesigned and validated GPR30-, p21, c-jun, and c-fos-siRNAs were obtained from Invitrogen. For controls, the cells were treated with Lipofectamine-2000 in Opti-MEM I medium without any siRNA as reagent control. Cells with scramble siRNA control (Invitrogen) and Lipofectamine-2000 in Opti-MEM I medium also were used.

Immunoprecipitation

The lysates of G-1–treated PC-3 cells and controls in lysis I buffer (Table S2, Supplemental Materials) with an equal amount of protein were incubated with antibody to phosphoserine/threonine/tyrosine residues. Protein A/G Plus-Agarose beads (Santa Cruz Biotechnology) were used to capture the complexes. The beads were heat-incubated with Laemmli sample buffer (Table S2, Supplemental Materials), and the supernatants were subjected to Western blot analysis.

Western blot analysis

After treatment, the cells were lysed in lysis II buffer (Table S2, Supplemental Materials). Five 20-μg protein lysates or immmunoprecipitates were run onto 10–12.5% polyacrylamide gels with SDS and transferred onto polyvinylidene fluoride membranes. Primary antibodies (Table S3, Supplemental Materials) were incubated with the membranes and recognized with horseradish peroxidase–conjugated secondary antibodies. ECL-Plus Western Blotting Detection Reagents (Amersham Biosciences, Piscataway, NJ) were used to visualize the complexes.

Immunofluorescence staining

PC-3 cells were cultured overnight in RPMI1640 medium supplemented with CS-FBS and then treated with 1 μM G-1 for 5 min to 24 h. The cells were immunostained with antibody to phosphorylated Erk1/2 recognized by FITC-conjugated secondary antibody. The nuclei were stained with DAPI. The stained cells were visualized by immunofluorescence microscopy.

Soft-agar growth assay

A 1-week 96-well soft-agar growth assay was performed as previously described (22). Briefly, a mixture of 25 μl of 37°C prewarmed 2 × RPMI1640 medium with CS-FBS and 25 μl 56°C prewarmed 1.2% Bacto™ Agar Select (BD Biosciences, San Jose, CA) was plated onto each well of a 96-well microplate. The solidified agar layer was topped with a mixture of 10 μl of cell suspension (7×10^3 cells), 20 μl of 2 × of the culture medium, and 30 μl of 0.8% Bacto™ Agar Select in the presence of 11.25 pmole of siRNA targeting GPR30 or scrambled Sheath™ negative RNAi control with Lipofectamine-2000 in Opti-MEM I medium. Semisolid feeder layer containing 25 μl of 2 × of the culture medium, and 25 μl of 1.2% Bacto™ Agar Select was added on the top of the solidified cell layer in each well. Each treatment was conducted in octuplicate. The cells were allowed to grow for 7 days, and the growth was determined by the Invitrogen AlamarBlue cell viability assay in accordance with the manufacturer's protocol. Fresh medium (100 μl) was placed on top of the layer for 10 min and then removed to maintain the moisture of the layer. Absorbance at 570 nm and

600 nm in each well was measured with the Perkin Elmer Victor microplate reader. Relative cell growth on soft agar was presented as the percentage difference in reduction of AlamarBlue between test and control cells, calculated as [(O2 × A1)−(O1 × A2)]/[(O2 × P1)−(O1 × P2)] × 100, where O1 is the molar extinction coefficient (E) of oxidized AlamarBlue at 570 nm (i.e., 80586), O2 is E of oxidized AlamarBlue at 600 nm (i.e., 117216), A1 and A2 are absorbance at 570 nm and 600 nm, respectively, of the well with GPR30 siRNA or control siRNA plus G-1–treated cells or G-1–treated cells, and P1 and P2 are absorbance at 570 nm and 600 nm, respectively, of the well with control ethanol-treated cells.

Xenograft experiments

PC-3 cells (1×10^6) in 100 μl of PBS were injected subcutaneously into the left and right sides of the flank of surgically castrated nude (*nu/nu)* athymic male mice (6 weeks of age, 24–29 g) (Taconic Laboratory, Hudson, NY). Tumor volumes were expressed in mm^3: volume (mm^3) = long diameter (mm) × short diameter $(mm)^2 \times 0.5236$. Mice with tumors of ~150 mm^3 were treated daily with vehicle alone (2.5% DMSO, 5% ethanol) or G-1 in vehicle (4 mg/kg/day) administered by subcutaneous injection (n=5). Tumors were measured every 4 days. At 12 days, mice were sacrificed and weighed after xenografts were removed.

Supplementary Material

Refer to Web version on PubMed Central for supplementary material.

Acknowledgements

We thank the Hong Kong Competitive Earmarked Research Grants/General Research Funds of University Grants Committee to K.M.L.; the Chinese University of Hong Kong Directed Grants for Research to K.M.L. and C.F.N.; and the U.S. National Institutes of Health awards ES006096, ES015584, CA015776, and CA112532 to S.-M.H for their financial supports in this study. We also thank Nancy K. Voynow for her professional editing for this manuscript.

References

1. Moriarty K, Kim KH, Bender JR. Minireview: estrogen receptor-mediated rapid signaling. Endocrinology. 2006; 147:5557–5563. [PubMed: 16946015]
2. Hammes SR, Levin ER. Extranuclear steroid receptors: nature and actions. Endocr. Rev. 2007; 28:726–741. [PubMed: 17916740]
3. Chambliss KL, Yuhanna IS, Anderson RG, Mendelsohn ME, Shaul PW. ERbeta has nongenomic action in caveolae. Mol. Endocrinol. 2002; 16:938–946. [PubMed: 11981029]
4. Pedram A, Razandi M, Levin ER. Nature of functional estrogen receptors at the plasma membrane. Mol. Endocrinol. 2006; 20:1996–2009. [PubMed: 16645038]
5. Wang Z, Zhang X, Shen P, Loggie BW, Chang Y, Deuel TF. A variant of estrogen receptor-α, hER-α36: transduction of estrogen- and antiestrogen-dependent membrane-initiated mitogenic signaling. Proc. Natl. Acad. Sci. USA. 2006; 103:9063–9068. [PubMed: 16754886]
6. Filardo EJ, Quinn JA, Bland KI, Frackelton AR Jr. Estrogen-induced activation of Erk1/2-1 and Erk1/2-2 requires the G protein-coupled receptor homolog, GPR30, and occurs via trans-activation of the epidermal growth factor receptor through release of HB-EGF. Mol. Endocrinol. 2000; 14:1649–1660. [PubMed: 11043579]

7. Revankar CM, Cimino DF, Sklar LA, Arterburn JB, Prossnitz ER. A transmembrane intracellular estrogen receptor mediates rapid cell signaling. Science. 2005; 307:1625–1630. [PubMed: 15705806]
8. Thomas P, Pang Y, Filardo EJ, Dong J. Identity of an estrogen membrane receptor coupled to a G protein in human breast cancer cells. Endocrinology. 2005; 146:624–632. [PubMed: 15539556]
9. Vivacqua A, Bonofiglio D, Albanito L, Madeo A, Rago V, Carpino A, et al. 17beta-estradiol, genistein, and 4-hydroxytamoxifen induce the proliferation of thyroid cancer cells through the g protein-coupled receptor GPR30. Mol. Pharmacol. 2006; 70:1414–1423. [PubMed: 16835357]
10. Vivacqua A, Bonofiglio D, Recchia AG, Musti AM, Picard D, Andò S, et al. The G protein-coupled receptor GPR30 mediates the proliferative effects induced by 17beta-estradiol and hydroxytamoxifen in endometrial cancer cells. Mol. Endocrinol. 2006; 20:631–646. [PubMed: 16239258]
11. Albanito L, Madeo A, Lappano R, Vivacqua A, Rago V, Carpino A, et al. G protein-coupled receptor 30 (GPR30) mediates gene expression changes and growth response to 17beta-estradiol and selective GPR30 ligand G-1 in ovarian cancer cells. Cancer Res. 2007; 67:1859–1866. [PubMed: 17308128]
12. Prossnitz ER, Oprea TI, Sklar LA, Arterburn JB. The ins and outs of GPR30: A transmembrane estrogen receptor. J. Steroid. Biochem. Mol. Biol. 2008; 109:350–353. [PubMed: 18406603]
13. Teng J, Wang ZY, Prossnitz ER, Bjorling DE. The G protein-coupled receptor GPR30 inhibits human urothelial cell proliferation. Endocrinology. 2008; 149:4024–4034. [PubMed: 18467434]
14. Filardo EJ, Thomas P. GPR30: a seven-transmembrane-spanning estrogen receptor that triggers EGF release. Trends Endocrinol. Metab. 2005; 16:362–367. [PubMed: 16125968]
15. Ahola TM, Alkio N, Manninen T, Ylikomi T. Progestin and G protein-coupled receptor 30 inhibit mitogen-activated protein kinase activity in MCF-7 breast cancer cells. Endocrinology. 2002; 143:4620–4606. [PubMed: 12446589]
16. Madak-Erdogan Z, Kieser KJ, Kim SH, Komm B, Katzenellenbogen JA, Katzenellenbogen BS. Nuclear and extranuclear pathway inputs in the regulation of global gene expression by estrogen receptors. Mol. Endocrinol. 2008; 22:2116–2127. [PubMed: 18617595]
17. Otto C, Rohde-Schulz B, Schwarz G, Fuchs I, Klewer M, Brittain D, et al. G protein-coupled receptor 30 localizes to the endoplasmic reticulum and is not activated by estradiol. Endocrinology. 2008; 149:4846–4856. [PubMed: 18566127]
18. Bologa CG, Revankar CM, Young SM, Edwards BS, Arterburn JB, Kiselyov AS, et al. Virtual and biomolecular screening converge on a selective agonist for GPR30. Nat. Chem. Biol. 2006; 2:207–212. [PubMed: 16520733]
19. Maggiolini M, Vivacqua A, Fasanella G, Recchia AG, Sisci D, Pezzi V, et al. The G protein-coupled receptor GPR30 mediates c-fos up-regulation by 17beta-estradiol and phytoestrogens in breast cancer cells. J. Biol. Chem. 2004; 279:27008–27016. [PubMed: 15090535]
20. Berry SJ, Coffey DS, Walsh PC, Ewing LL. The development of human benign prostatic hyperplasia with age. J. Urol. 1984; 132(3):474–479. [PubMed: 6206240]
21. Cunha GR, Donjacour AA, Cooke PS, Mee S, Bigsby RM, Higgins SJ, et al. The endocrinology and developmental biology of the prostate. Endocr. Rev. 1987; 8:338–362. [PubMed: 3308446]
22. Ke N, Albers A, Claassen G, Yu DH, Chatterton JE, Hu X, et al. One-week 96-well soft agar growth assay for cancer target validation. Biotechniques. 2004; 36:826–833. [PubMed: 15152603]
23. Lau KM, LaSpina M, Long J, Ho SM. Expression of estrogen receptor (ER)-alpha and ER-beta in normal and malignant prostatic epithelial cells: regulation by methylation and involvement in growth regulation. Cancer Res. 2000; 60:3175–3182. [PubMed: 10866308]
24. Maity SN, de Crombrugghe B. Role of the CCAAT-binding protein CBF/NF-Y in transcription. Trends Biochem. Sci. 1998; 23:174–178. [PubMed: 9612081]
25. Yun J, Chae HD, Choy HE, Chung J, Yoo HS, Han MH, et al. p53 negatively regulates cdc2 transcription via the CCAAT-binding NF-Y transcription factor. J. Biol. Chem. 1999; 274:29677–29682. [PubMed: 10514438]
26. Yun J, Chae HD, Choi TS, Kim EH, Bang YJ, Chung J, et al. Cdk2-dependent phosphorylation of the NF-Y transcription factor and its involvement in the p53-p21 signaling pathway. J. Biol. Chem. 2003; 278:36966–36972. [PubMed: 12857729]

27. Chen RH, Sarnecki C, Blenis J. Nuclear localization and regulation of Erk1/2- and rsk-encoded protein kinases. Mol. Cell Biol. 1992; 12:915–927. [PubMed: 1545823]
28. Lenormand P, Pagès G, Sardet C, L'Allemain G, Meloche S, Pouysségur J. MAP kinases: activation, subcellular localization and role in the control of cell proliferation. Adv. Second Messenger Phosphoprotein Res. 1993; 28:237–244. [PubMed: 8398409]
29. Gonzalez FA, Seth A, Raden DL, Bowman DS, Fay FS, Davis RJ. Serum-induced translocation of mitogen-activated protein kinase to the cell surface ruffling membrane and the nucleus. J. Cell Biol. 1993; 122:1089–1101. [PubMed: 8394846]
30. Hill CS, Wynne J, Treisman R. Serum-regulated transcription by serum response factor (SRF): a novel role for the DNA binding domain. EMBO J. 1994; 13:5421–5432. [PubMed: 7957108]
31. Angel P, Karin M. The role of Jun, Fos and the AP-1 complex in cell-proliferation and transformation. Biochim Biophys Acta. 1991; 1072:129–157. [PubMed: 1751545]
32. Angel P, Hattori K, Smeal T, Karin M. The jun proto-oncogene is positively autoregulated by its product, Jun/AP-1. Cell. 1988; 55:875–885. [PubMed: 3142689]
33. van Dam H, Duyndam M, Rottier R, Bosch A, de Vries-Smits L, Herrlich P, et al. Heterodimer formation of cJun and ATF-2 is responsible for induction of c-jun by the 243 amino acid adenovirus E1A protein. EMBO J. 1993; 12:479–487. [PubMed: 8382609]
34. Pulverer BJ, Kyriakis JM, Avruch J, Nikolakaki E, Woodgett JR. Phosphorylation of c-jun mediated by MAP kinases. Nature. 1991; 353:670–674. [PubMed: 1922387]
35. Smeal T, Binetruy B, Mercola DA, Birrer M, Karin M. Oncogenic and transcriptional cooperation with Ha-Ras requires phosphorylation of c-Jun on serines 63 and 73. Nature. 1991; 354:494–496. [PubMed: 1749429]
36. Gupta P, Prywes R. ATF1 phosphorylation by the ERK1/2 MAPK pathway is required for epidermal growth factor-induced c-jun expression. J. Biol. Chem. 2002; 277:50550–50556. [PubMed: 12414794]
37. Carruba G, Pfeffer U, Fecarotta E, Coviello DA, D'Amato E, Lo Castro M, et al. Estradiol inhibits growth of hormone-nonresponsive PC3 human prostate cancer cells. Cancer Res. 1994; 54:1190–1193. [PubMed: 8118804]
38. Pandey DP, Lappano R, Albanito L, Madeo A, Maggiolini M, Picard D. Estrogenic GPR30 signalling induces proliferation and migration of breast cancer cells through CTGF. EMBO J. 2009; 28(5):523–532. [PubMed: 19153601]
39. Haas E, Bhattacharya I, Brailoiu E, Damjanović M, Brailoiu GC, Gao X, et al. Regulatory role of G protein-coupled estrogen receptor for vascular function and obesity. Circ Res. 2009; 104:288–291. [PubMed: 19179659]
40. Marshall CJ. Specificity of receptor tyrosine kinase signaling: transient versus sustained extracellular signal-regulated kinase activation. Cell. 1995; 80:179–185. [PubMed: 7834738]
41. Stanciu M, DeFranco DB. Prolonged nuclear retention of activated extracellular signal-regulated protein kinase promotes cell death generated by oxidative toxicity or proteasome inhibition in a neuronal cell line. J. Biol. Chem. 2002; 277:4010–4017. [PubMed: 11726647]
42. Tang D, Wu D, Hirao A, Lahti JM, Liu L, Mazza B, et al. ERK1/2 activation mediates cell cycle arrest and apoptosis after DNA damage independently of p53. J. Biol. Chem. 2002; 277:12710–12717. [PubMed: 11821415]
43. Adachi T, Kar S, Wang M, Carr BI. Transient and sustained ERK1/2 phosphorylation and nuclear translocation in growth control. J. Cell. Physiol. 2002; 192:151–159. [PubMed: 12115721]
44. Chen JR, Plotkin LI, Aguirre JI, Han L, Jilka RL, Kousteni S, et al. Transient versus sustained phosphorylation and nuclear accumulation of ERK1/2s underlie anti-versus pro-apoptotic effects of estrogens. J. Biol. Chem. 2005; 280:4632–4638. [PubMed: 15557324]
45. Abukhdeir AM, Park BH. P21 and p27: roles in carcinogenesis and drug resistance. Expert Rev. Mol. Med. 2008; 10:e19. [PubMed: 18590585]
46. Dulić V, Stein GH, Far DF, Reed SI. Nuclear accumulation of p21Cip1 at the onset of mitosis: a role at the G2/M-phase transition. Mol. Cell. Biol. 1998; 18:546–557. [PubMed: 9418901]
47. Pumiglia KM, Decker SJ. Cell cycle arrest mediated by the MEK/mitogen-activated protein kinase pathway. Proc. Natl. Acad. Sci. USA. 1997; 94:448–452. [PubMed: 9012803]

48. Dangi S, Chen FM, Shapiro P. Activation of extracellular signal-regulated kinase (ERK1/2) in G2 phase delays mitotic entry through p21(WAF1/CIP1)CIP1. Cell Prolif. 2006; 39:261–279. [PubMed: 16872362]

49. Davis JN, Singh B, Bhuiyan M, Sarkar FH. Genistein-induced upregulation of p21(WAF1/CIP1)WAF1, downregulation of cyclin B, and induction of apoptosis in prostate cancer cells. Nutr. Cancer. 1998; 32:123–131. [PubMed: 10050261]

50. Prasad S, Kaur J, Roy P, Kalra N, Shukla Y. Theaflavins induce G2/M arrest by modulating expression of p21(WAF1/CIP1)waf1/cip1, cdc25C and cyclin B in human prostate carcinoma PC-3 cells. Life Sci. 2007; 81:1323–1331. [PubMed: 17936851]

51. Zwicker J, Lucibello FC, Wolfraim LA, Gross C, Truss M, Engeland K, et al. Cell cycle regulation of the cyclin A, cdc25C and cdc2 genes is based on a common mechanism of transcriptional repression. EMBO J. 1995; 14:4514–4522. [PubMed: 7556094]

52. Manni I, Mazzaro G, Gurtner A, Mantovani R, Haugwitz U, Krause K, et al. NF-Y mediates the transcriptional inhibition of the cyclin B1, cyclin B2, and cdc25C promoters upon induced G2 arrest. J. Biol. Chem. 2001; 276:5570–5576. [PubMed: 11096075]

53. Hu Q, Lu JF, Luo R, Sen S, Maity SN. Inhibition of CBF/NF-Y mediated transcription activation arrests cells at G2/M phase and suppresses expression of genes activated at G2/M phase of the cell cycle. Nucleic Acids Res. 2006; 34:6272–6785. [PubMed: 17098936]

54. Kardassis D, Papakosta P, Pardali K, Moustakas A. c-Jun transactivates the promoter of the human p21 gene by acting as a superactivator of the ubiquitous transcription factor Sp1. J. Biol. Chem. 1999; 274:29572–29581. [PubMed: 10506225]

55. Livak KJ, Schmittgen TD. Analysis of relative gene expression data using real-time quantitative PCR and the 2(−delta delta C(T)) method. Methods. 2001; 25:402–408. [PubMed: 11846609]

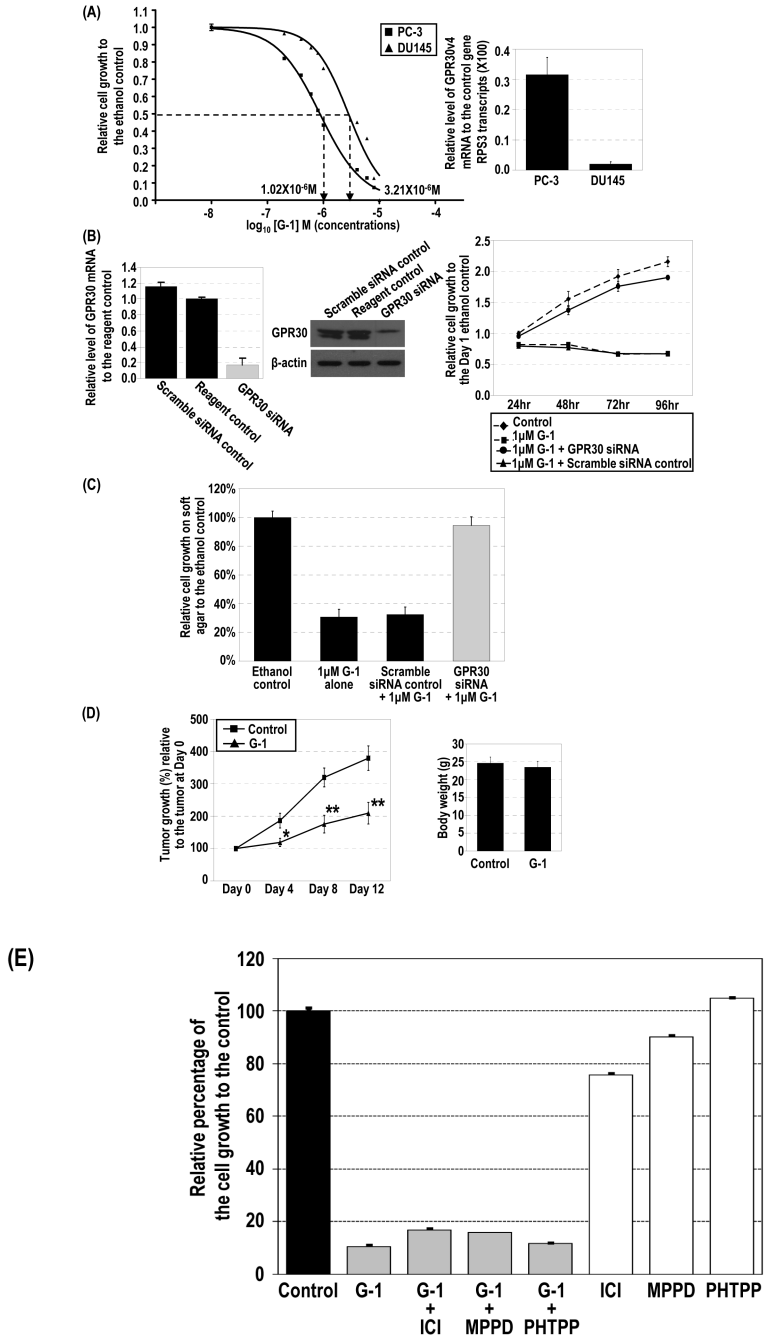

Figure 1.

G-1–induced inhibition of cell growth via G2/M arrest and relative expression of GPR30 mRNA in PCa cells. (A) PC-3 (■) and DU145 (▲) cells were treated with 10^{-8}–10^{-5} M G-1 for 4 days, and control cells were treated with ethanol. Cell growth relative to that of the control at day 4 was plotted against the concentrations of G-1 with sigmoid curve fitting, and the IC_{50} was determined. Levels of expression of GPR30 mRNA in PC-3 and DU145 cells were quantified by real-time RT-PCR analysis. (B) siRNA specifically reduced GPR30 expression as determined by real-time RT-PCR analysis and Western blot analysis. PC-3

cells were treated with 1 μM G-1 for 4 days in the presence of GPR30 siRNA or scramble siRNA as a control. Two reagent controls with ethanol and with G-1 were included. The growth of the cells relative to that of the ethanol control at day 1 was determined. (C) G-1 inhibited anchorage-independent growth via GPR30-mediated signaling. Relative cell growth on soft agar to the ethanol-treated control cells for G-1–treated PC-3 cells with either GPR30 siRNA or scramble control siRNA are presented. (D) G-1 inhibited tumor growth of PC-3 xenografts in vivo. The percentage of tumor growth relative to the original size of the tumors at day 0 in the G-1–treated mice (▲) and control mice (■) and the body weights of mice after removal of xenografts are presented. *, $p<0.05$; **, $p<0.005$. (E). PC-3 cells were treated with 1 μM G-1 for 4 days in the presence of 1 μM ER antagonists (ICI 182,780 [ICI], MPP dihydrochloride [MPPD] and PHTPP. Cell growth relative to that of the ethanol control at day 4 is presented. The cell growth for the ethanol control was set as 1. Column, mean; bar, standard deviation.

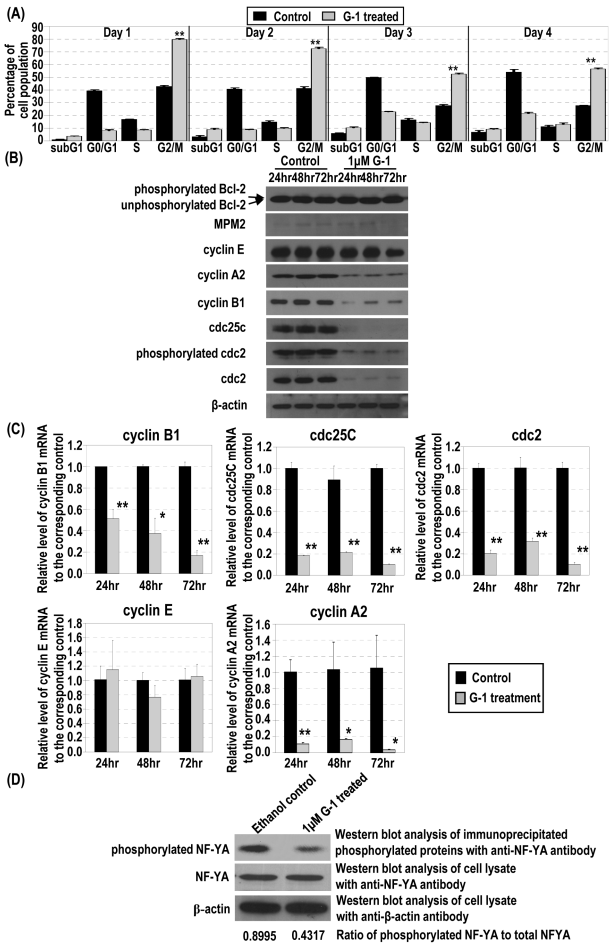

Figure 2.

Effects of G-1 on expression of cell-cycle regulators and markers and NF-YA phosphorylation. (A) Percentages of PC-3 cells treated or not treated with 1 μM G-1 at different cell-cycle phases were determined by flow cytometry. (B) The lysates of PC-3 cells treated with 1 μM G-1 or ethanol were subjected to Western blot analysis to determine the protein level of phosphorylated bcl-2, MPM2, cyclin E, cyclin A2, cyclin B1, cdc25C, phosphorylated cdc2, total cdc2, and β-actin. (C) Cells were subjected to real-time RT-PCR analysis to determine mRNA levels. *, $p<0.01$; **, $p<0.001$. (D) The cell lysates were immunoprecipitated with antibody to phosphoserine/threonine/tyrosine residues. Levels of NF-YA protein in the immunoprecipitates were determined by Western blot analysis. The levels of β-actin protein were used as loading control for immunoprecipitation. Ratio of phosphorylated NF-YA to total NF-YA for ethanol and G-1 treated cells are presented.

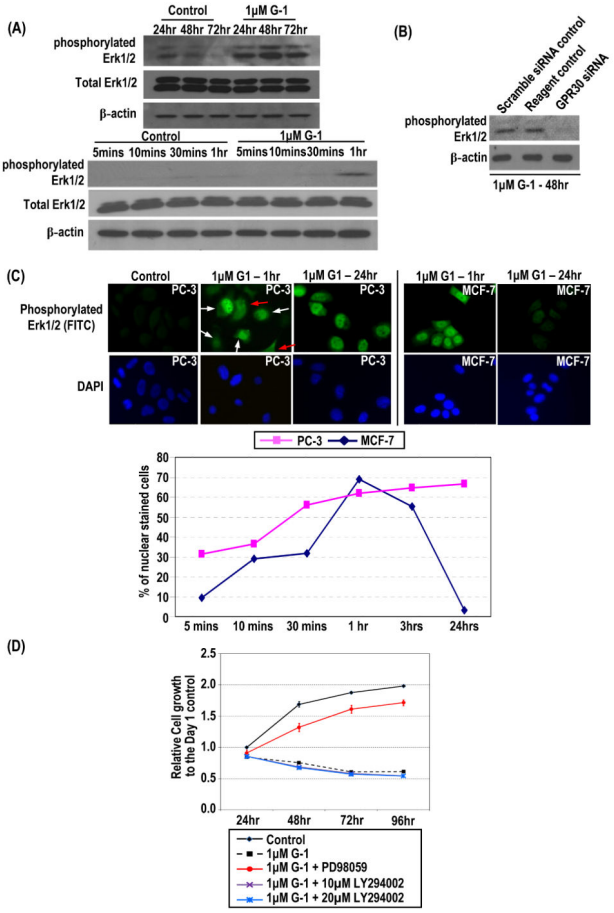

Figure 3.

G-1 induced rapid and sustained Erk1/2 phosphorylation with nuclear accumulation of phosphorylated Erk1/2. (A) PC-3 cells treated with 1 μM G-1 or ethanol for 3 days. Cells were lysed at early (5 min–1 h) and late (24–72 h) time points, and levels of total and phosphorylated Erk1/2 and β-actin protein were determined by Western blot analysis. (B) siRNA-treated PC-3 cells (GPR30 siRNA) and controls (scramble siRNA control and reagent control), all treated with 1 μM G-1, were lysed, and levels of phosphorylated Erk1/2 and β-actin protein were determined by Western blot analysis. (C) PC-3 and MCF-7 cells treated with 1 μM G-1 from 5 min to 24 h. Antibody to phosphorylated Erk1/2 was used for immunofluorescence staining (green). The nuclei were stained with DAPI (blue). Representative micrographs of the 1 h– and 24 h–treated PC-3 and MCF7 cells and ethanol-treated PC-3 cells are shown. White arrows indicate cells with nuclear accumulation of phosphorylated Erk1/2; red arrows indicate cells with diffuse cytoplasmic staining. Cells with and without nuclear staining were counted, and the percentage of nuclear-stained cells from 5 min to 24 h were determined. (D) The growth of the cells treated with PD98059/LY294002 and G-1 relative to that of the ethanol control at day 1 was determined. The G-1-treated cells without pretreatment with PD98059/LY294002 and the ethanol-treated cells were used as controls.

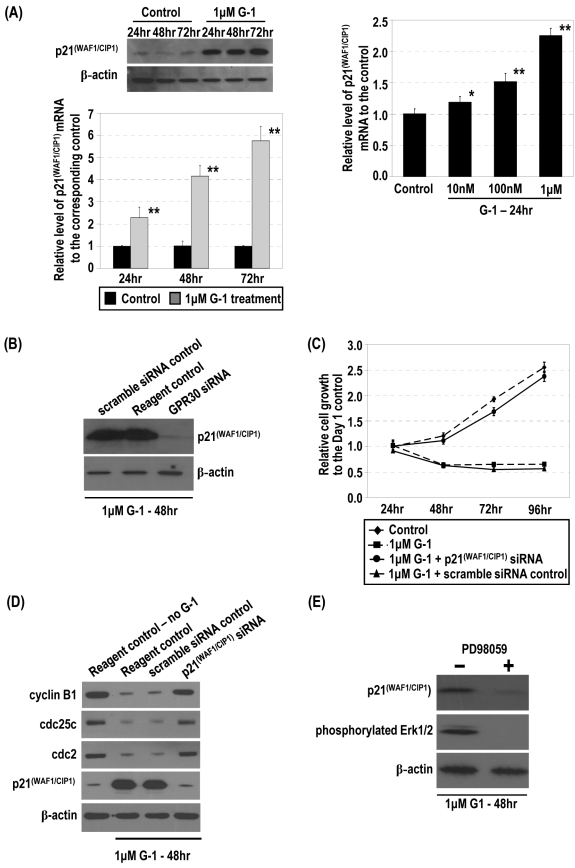

Figure 4.

G-1 induced p21 mRNA and protein via GPR30 and downregulation of expression of G2 checkpoint regulators for inhibition of cell growth by p21. (A) PC-3 cells were treated with 1 μM G-1 or ethanol. Levels of p21 protein and mRNA were determined by Western blot and real-time RT-PCR analyses, respectively. Furthermore, the cells were treated with 10^{-8}–10^{-6} M G-1. Levels of p21 mRNA in cells were quantified by real-time RT-PCR analysis. *, $p<0.01$; **, $p<0.001$. (B) The siRNA-treated cells (GPR30siRNA) and controls (scramble siRNA control and reagent control), all treated with 1 μM G-1, were lysed and the levels of p21 and β-actin protein determined by Western blot analysis. (C) The G-1–treated cells with p21 siRNA or the scramble siRNA control were subjected to Western blot analysis to determine levels of cyclin B1, cdc25c, cdc2, p21, and β-actin protein. Two reagent controls (ethanol or 1 μM G-1) were included. (D) Effects of p21siRNA knockdown on the G-1–induced inhibition of cell growth are presented with the controls. Growths of the cells relative to that of the ethanol control at day 1 were determined. (E) G-1–induced expression of p21 was dependent on Erk1/2 activation. PC-3 cells were treated with 1 μM G-1 for 48 h in the presence or absence of 30 μM PD98059. The levels of p21 and β-actin protein were determined by Western blot analysis.

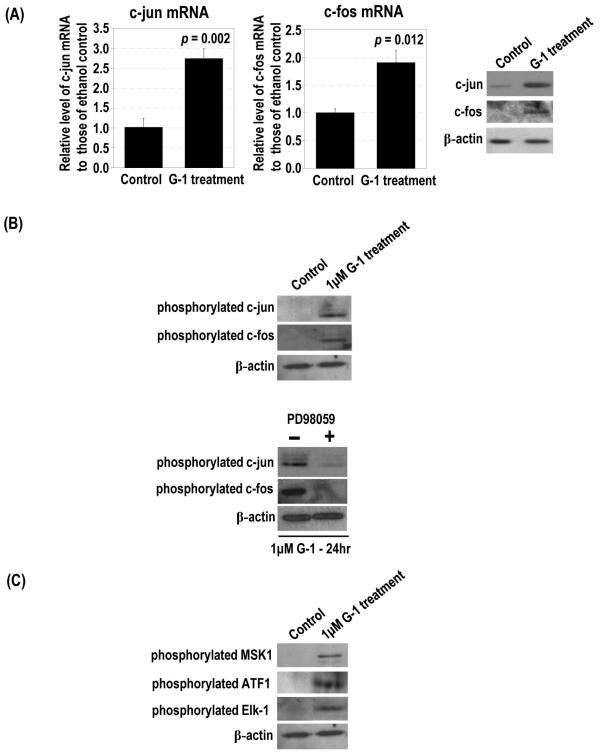

Figure 5.

G-1 upregulated c-jun and c-fos expression and phosphorylation and activated upstream regulators of c-jun. PC-3 cells were treated with 1 μM G-1. (A) The levels of c-jun and c-fos mRNA and protein in G-1–treated cells and ethanol-treated controls were determined by real-time RT-PCR and Western blot analyses, respectively. The levels of β-actin protein were used as the loading control. (B) PC-3 cells were treated with 1 μM G-1 in the presence and absence of 30 μM PD98059. The ethanol-treated cells were used as the control. The levels of phosphorylated c-jun and phosphorylated c-fos proteins in the cells were determined by Western blot analysis. (C) The levels of phosphorylated MSK1, ATF1, and Elk-1 in G-1– and ethanol-treated cells were determined by Western blot analysis.

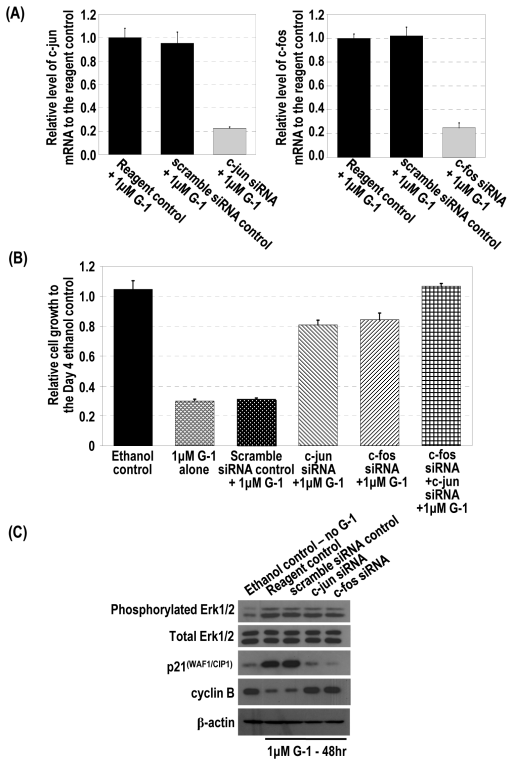

Figure 6.

siRNA knockdown of c-jun and c-fos blocked the G-1 induced inhibition of cell growth, upregulation of p21, and downregulation of cyclin B but showed no effect on G-1–induced phosphorylation of Erk1/2. (A) siRNA specifically reduced c-jun or c-fos expression as determined by real-time RT-PCR analysis. (B) PC-3 cells were treated with 1 μM G-1 for 4 days in the presence of c-jun siRNA, c-fos siRNA, or scramble siRNA as a control. Two reagent controls with ethanol and with G-1 without any siRNA were included. The growth of the cells relative to that of the ethanol control at day 1 was determined. (C) The G-1–treated cells with c-jun siRNA, c-fos siRNA, or the scramble siRNA control were subjected to Western blot analysis to determine levels of phosphorylated Erk1/2, p21, cyclin B1, and β-actin protein. Two reagent controls (ethanol or 1 μM G-1) without any siRNA were included.

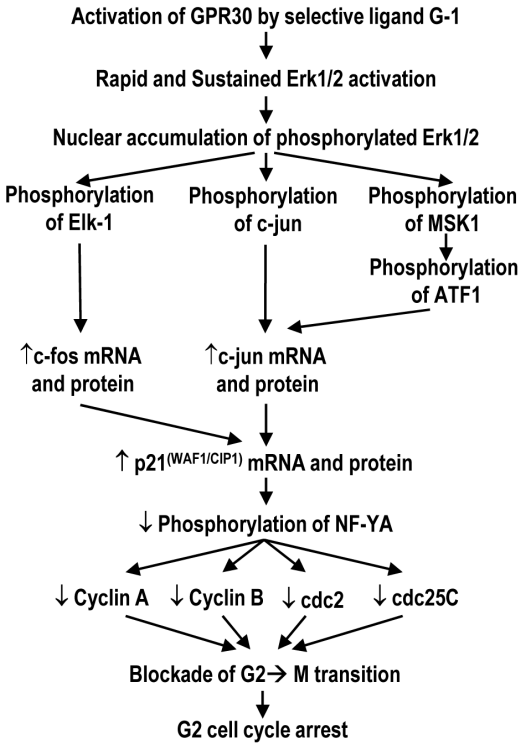

Figure 7.
Proposed GPR30-mediated signaling by G-1 in prostate cancer cells for cell growth inhibition.